King Saud University

**Journal of King Saud University –
Computer and Information Sciences**

www.ksu.edu.sa
www.sciencedirect.com

ORIGINAL ARTICLE

Measurement of changes in glacier extent in the Rimo glacier, a sub-range of the Karakoram Range, determined from Landsat imagery

Prashant Kumar *, Amol P. Bhondekar, Pawan Kapur

Central Scientific Instruments Organisation (CSIO), CSIR, Sector-30C, Chandigarh 160030, India

Abstract   Accurate estimation of the spatiotemporal surface dynamics is very important for natural resource planning. This paper discusses a novel approach for the study of the surface patterns of a particular glacier Rimo located at 35°21′21″N77°22′05″E, about 20 km northeast of the snout of Siachen. Change detection in multiple images of the same location taken at different time intervals are of widely circulated use due to a large number of applications in various disciplines such as climate change, remote sensing and so on. The proposed technique uses image processing to derive regression models of selected glacier segments, these models are then used to measure area under the curve to estimate the surface area changes of the glacier. The surface area changes thus obtained have also been validated by standard method of pixel counting. With the rise in the global warming, the net change in the surface area of the concerned glacier is estimated using statistical analysis from 1998 to 2011. The results obtained show a fair degree of accuracy as compared to the standard method of pixel counting. We also discuss important pre-processing methods used in extracting the final concerned region of interest from a large satellite imagery of fairly average resolution.

© 2013 Production and hosting by Elsevier B.V. on behalf of King Saud University.

1. Introduction

World's freshwater prime source is cryosphere which stores 75% of the freshwater. Changes in sea level are caused mainly due to changes in ice mass. On a territorial order, freshwater availability depends primarily on glaciers and ice caps (IPCC, 2007). Freshwater availability for various purposes such as irrigation, domestic use, mountain diversion, animals and plants that depend on melting of glacier, is majorly affected by the retreat of glaciers. The extended glacier retreats will cause a number of quantitative wallops. There are many areas which are dependent on water released due to the retreat of glaciers during the hot summer seasons. If the glacier keeps on melting at the rate as it is melting in the present scenario then eventually many glacial ices will be wiped out causing severe situations for human beings. Such a decrease in water runoff will have an effect on the irrigation capabilities and will decrease the stream flows essential to keep water reservoirs refilled (Warning, 2012).

* Corresponding author. Tel.: +91 7814047689.
  E-mail address: pras.santu@gmail.com (P. Kumar).

The Siachen glacier has been retreating for the last 30 years according to the findings of Pakistan Meteorological Department in 2007 and is retreating at an alarming rate (Gupta, 2008). The glacier size has depleted by almost 35% and is melting at a rate of about 110 m a year as indicated from the studies of the satellite images (Sadangi, 2007; Rao, 2011). The glacier has depleted nearly 800 m (Kapadia, 1998) in a 11 year duration and the measure of retreat is 1700 m in 17 years period. Moran has estimated that Siachen glaciers will shrink to 20% of their current size by 2035 (Moran, 2011). Global warming is the most cited reason for the recent glacial retreat. The various construction and excavation activities have played a vital role in contributing towards global warming thereby causing the retreat of glaciers such as oil pipelines laid by India in 2001 inside the glacier for almost 250 km to provide kerosene oil and aviation fuels to the frontier outstations from base camps (Asad Hakeem, 2007).

Although the satellite imagery and topographic information can be used for glacier mapping, interpreting causal mechanisms for changing glacial boundary conditions and climate is difficult, as there is a significant disconnect between information on boundary conditions and process mechanics. Therefore, information integration and computer-assisted approaches to glacier mapping, parameter estimation, and numerical modelling are required to produce reliable results that go beyond traditional techniques (Bishop et al., 2007). Satellite remote sensing is a practical approach used in the assessment of glacier retreat. There are many remote sensing methods available for quantification of the glacier retreat. These methods include elevation changes observations, ice flux estimations, spatial extent change measurement, snowline elevation and accumulation–ablation area ratio calculations (Bamber and Rivera, 2007). Digital change detection is one of the popular processes in remote sensing applications aimed at identifying spatiotemporal surface dynamics (Coppin et al., 2004). Wherein, images acquired on the same geographical area at different time intervals are used for the analysis. Data transformation operations and analysis techniques are used to characterise various change detection methods to describe the area of substantial variability. A variety of digital change detection algorithms have been developed so far viz. background subtraction, image ratioing, image differencing, image regression, monotemporal change delineation, multitemporal linear data transformation, delta classification, multidimensional temporal feature analysis, change vector analysis, composite analysis and multitemporal biomass index (Singh, 1989). Measurements of the glacial retreat have been done by several researchers through different techniques (Bolch and Menounos, 1985; Karimi et al., 1955; Moholdt and Nuth, 2010; Klein and Isacks, 1999; Mas, 1999; Venteris, 1999; Paul et al., 2004, 2007; Bartholom and Belward, 2005; Khromova et al., 2006; Berthier et al., 2007; Mihalcea et al., 2008; Moran, 2011; Rao, 2011).

Rimo is a glacier which has been retreating over the period of time causing a danger for water scarcity in the nearby region. Until twentieth century, Rimo was an unknown and unvisited place. Due to various human activities going on in Rimo glacial region, the total surface area of Rimo glacier has reduced significantly since the end of the 19th century. There has been an increase in the glacier retreat rates and mass imbalance losses in the Siachen and nearby glaciers.

This work presents a novel technique for surface area change estimation of Rimo glacier based on monotemporal image regression, wherein standard image pre-processing techniques viz. intensity normalisation, registration and edge detection are applied to create temporal skeletal images. The skeletal segments of each temporal skeletal image are then segmented and regressed to obtain polynomial models of various orders. The multitemporal polynomial curves for each segment are then superimposed on each other and the area enclosed among them is calculated using integrals. The proposed methodology has been addressed as Integral Method (IM) henceforth. In the present study, the segmentation has been done manually which may be automated and invites research interests for optimum segment selection parameters. The results thus obtained by IM are comparable with the results of standard pixel counting method (PCM).

2. Methodology

Landsat 5 digital imagery were taken and studied for three time periods 1998, 2005 and 2011. The important steps in the proposed technique are input image description, cropping the area of study, intensity normalisation, radiometric correction, registration, skeleton formation, change detection, application of a statistical regression model for functional mapping of the segments of the mountain and finally estimation of the net shift in the area using definite integrals and PCM for accuracy assessment. Fig. 1 shows the schema of the steps involved in the pre-processing, modelling and validation. The proposed technique was implemented using image processing toolbox of MATLAB and custom scripts.

2.1. Study area characterisation

Rimo is the name of the glacier chosen for study purpose. It rests in the northern part of the Rimo Muztagh which is a sub range of the Karakoram Range and is located about 20 km northeast of the snout of the Siachen Glacier. The area is located at 35°21′21″N77°22′05″E. Fig. 2 shows the map of study area Rimo glacier. Karakoram Range is more glaciated in comparison to the Himalaya and European Alps. Glaciations and recession of mountain glaciers with long-term changes in temperature may signal climate change. Karakoram glaciers have been found mostly slugging according to a study done by the Universities of California and Potsdam, because many Karakoram glaciers are covered with junks produced as a result of various natural phenomena and human activities and it has insulated the ice from the warmth of the sun. The retreat rate is alarming wherever there is no such insulation.

2.2. Image processing

2.2.1. Input image characterisation

Input image is a grayscale satellite image. The input image is shown in Fig. 3 with area of interest circled in red colour Landsat 5 thematic mapper images have been taken for the study purpose. Landsat 5 TM image data files consist of seven spectral bands. The band channel is 5 as it is very sensitive to moisture content and is also good at differentiating between clouds and snow. The resolution is 30 m. Due to different acquisition dates and atmospheric conditions, scene differences exist in the
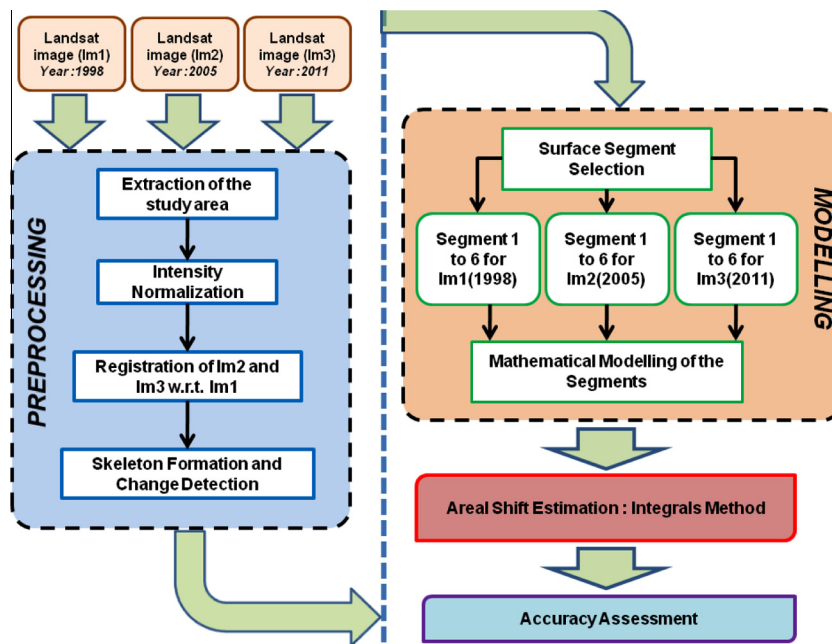
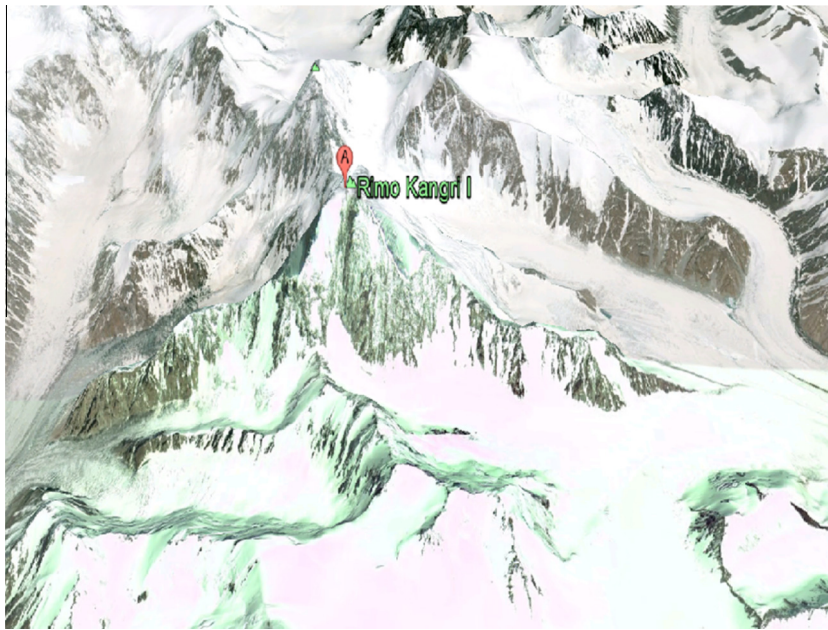**Figure 1** Workflow diagram of the technique.

Figure 2 Study map of Rimo glacier.

imageries acquired over a large geographic region. Therefore this kind of satellite data is most suitable for the analysis of relatively small geographic areas (Sawaya et al., 2003). The image acquisition dates are chosen with a view of the change detection algorithms to be used for the purpose (Coppin and Bauer, 1996). Therefore, three cloud-free images corresponding to Landsat 5 TM of the concerned region have been taken for each of the years 1998, 2005 and 2011 from US Geological Survey (Path/Row – 147/35) in the time period ranging from August to October because of the availability of the rimo images

in the database of US Geological Survey. The images are shown in Fig. 4(a/b/c).

2.2.2. Cropping of study area

The particular area is extracted in the form of the rectangular image of size 350×250 pixels. The area of interest is surrounded by the coordinates in the clockwise order as given in the order of '35.90 N, 77.38E', '35.84 N, 77.45E', '35.75 N, 77.40E', '35.78 N, 77.34E'. The cropped area is shown in Fig. 4(d/e/f).
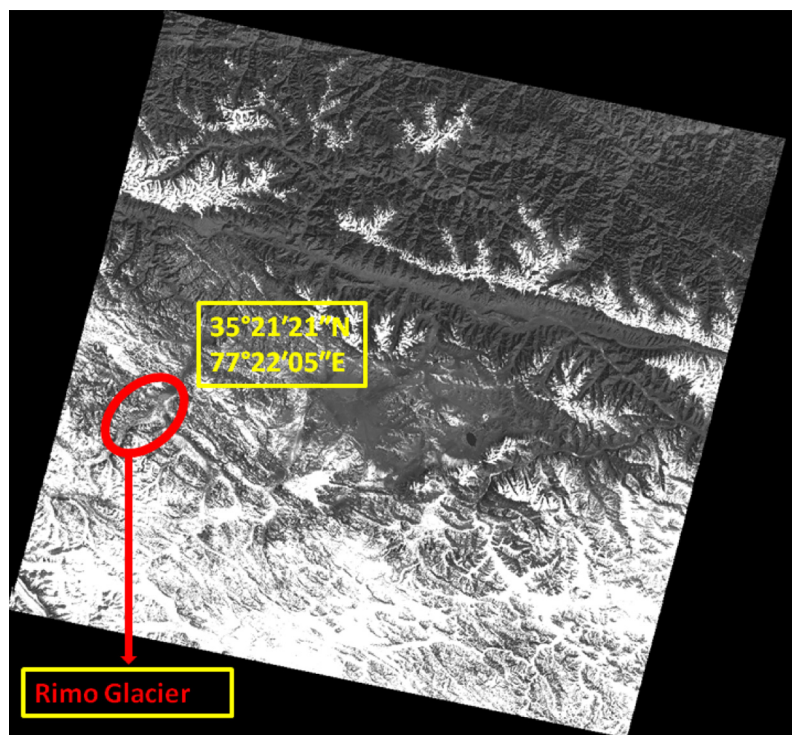
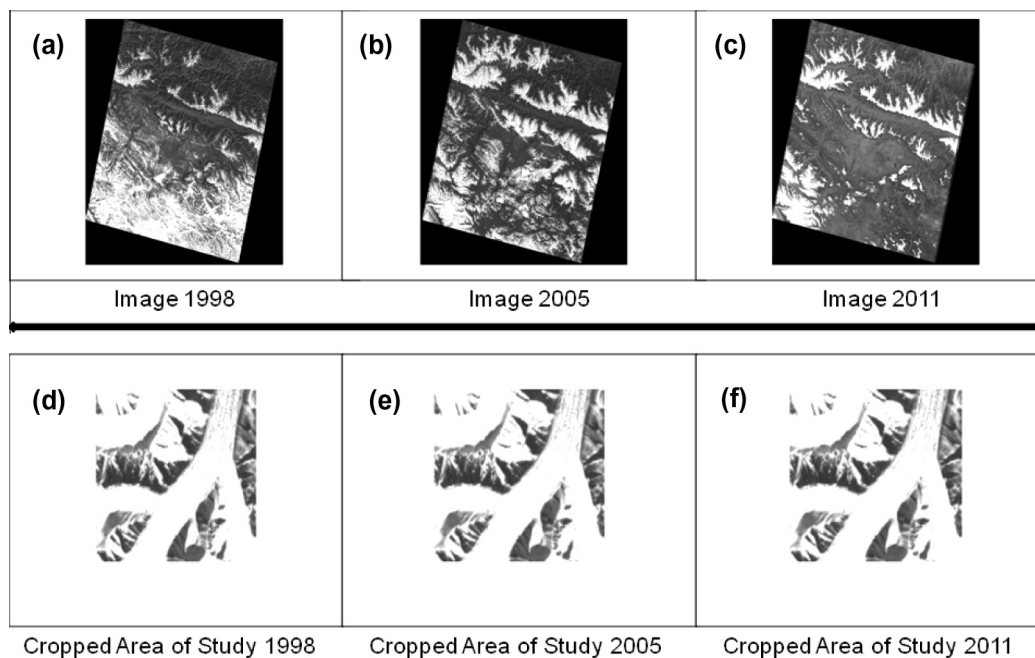**Figure 3** Input image with area of interest in red circle.

Figure 4 Landsat images of Rimo glacier for the years (a) 1998, (b) 2005 and (c) 2011 and the corresponding cropped images of the actual study site for the years (d) 1998, (e) 2005 and (f) 2011.

2.2.3. Intensity normalisation and radiometric calibration

Intensity normalisation is an operation which increases the contrast of an image by enhancing the dynamic range of intensity values given to pixels with the most probable intensity values. In the intensity normalisation operation that is used to produce the results shown in this paper, the transformation is scaled such that the minimum value of intensity in the original image is represented as zero intensity value in the normalised image, and, the maximum value of intensity in the original image is represented as intensity value that is equal
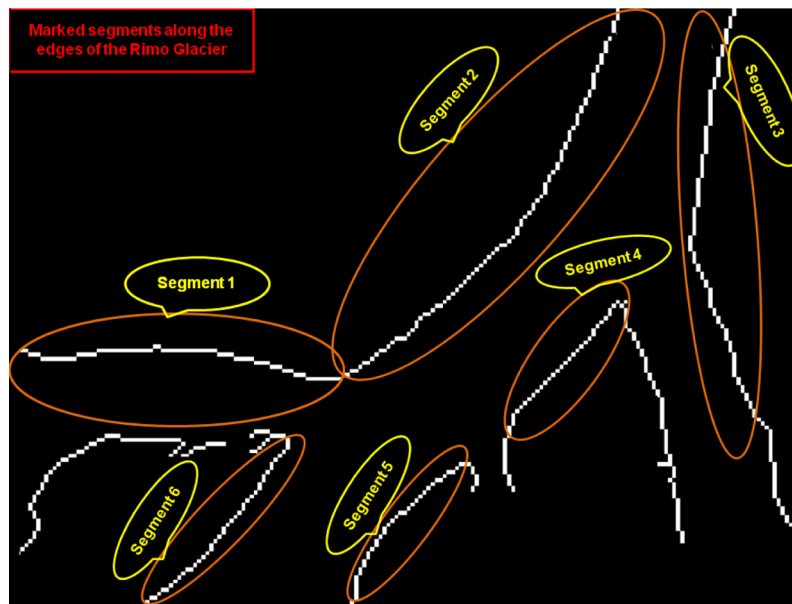
Figure 5   Skeletal image of the study region along with identified segments.

(a) XOR Year: 1998-2005   (b) XOR Year: 2005-2011

Figure 6   Changes detected by XOR Operation of (a) Im1 (1998) and Im2 (2005) and (b) Im2 (2005) and Im3 (2011).

to the maximum intensity (255) value determined by the bit depth (8-bit) of the image. This yields results that have a dynamic range that is similar to the one produced by the histogram equalisation algorithm (Gonzalez et al., 2009).

Generally, the absorption and scattering effects due to atmosphere are not required to be corrected in a detailed manner and often adjunct information such as visibility and relative humidity is not easily available. Therefore, if the atmosphere effects are considered to be a problem in imagery, approximate rectification is carried out for the bulk correction of the atmospheric effects. Here it is assumed that for each scene, each band of data must have some pixels close to zero brightness value but it is never zero because of the effects of the atmosphere such as path radiance. Now when the histograms are drawn for each band,

the lowest brightness value will be non-zero. Moreover due to Mie scattering, the lowest brightness value will be away from the origin for the lower wavelength. Further the amount by which each histogram has shifted in the brightness away from the origin is calculated and correction is done by subtracting this amount from each pixel brightness in that band (Richards and Jia, 2010).

2.2.4. Geometric correction and image registration

There are various techniques to correct the geometric distortion present in the digital data. Modelling the nature and magnitude of the sources of distortion and using these models to establish the correction formulae is one of the most optimised method but this technique is effective when types of the distor-
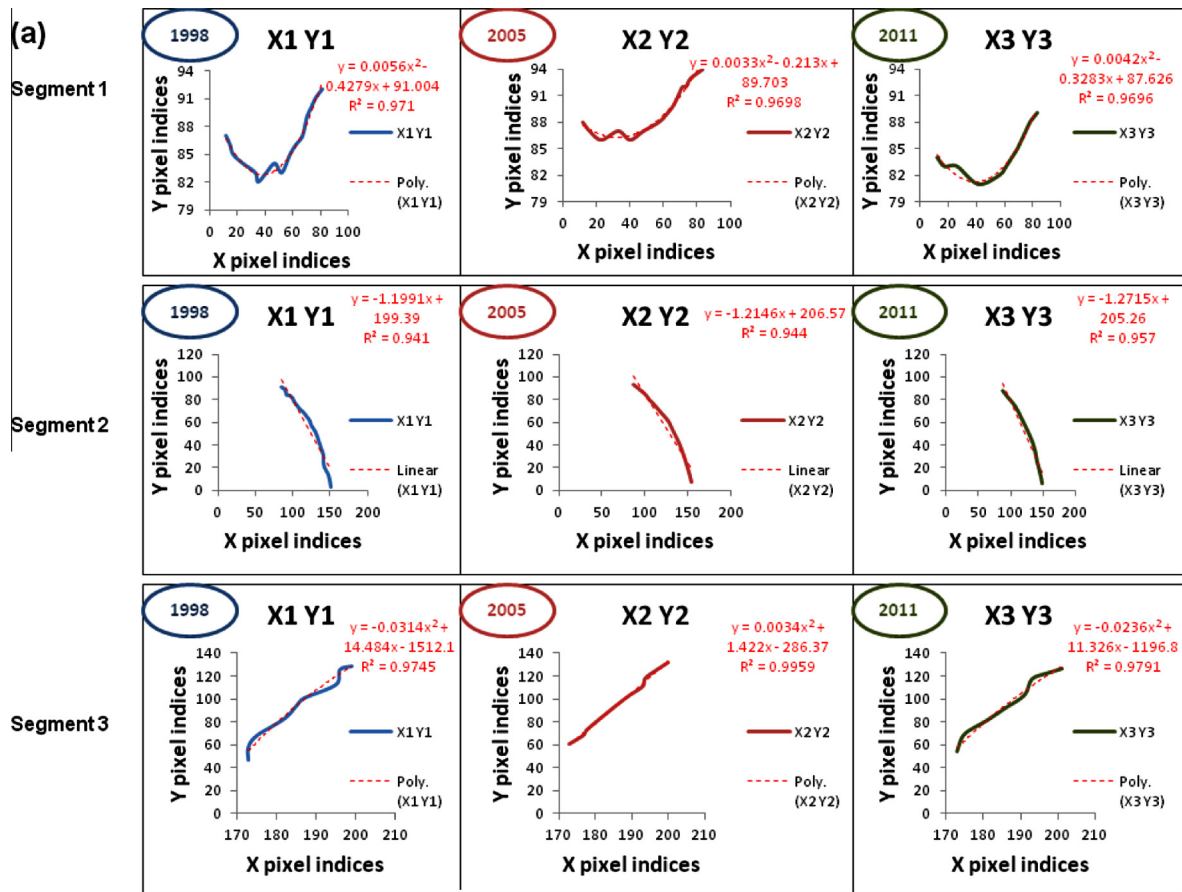
Figure 7 Polynomial equations of the best fit curves for segments 1, 2 and 3 for each of the three years (1998, 2005 and 2011).

tion are well characterised, such as caused by earth rotation (Richards and Jia, 2010). The approach used here for geometric correction depends upon finding the correlations between the addresses of pixels in an image and the corresponding coordinates of those points on the ground via a map. These correlations are used to rectify the image geometry regardless of the knowledge of the source and type of distortion.

Here we have three images and the first image (Image of 1998) is considered as the base image with respect to which, changes have been detected further. The images of 1998, 2005 and 2011 have been represented as Im1, Im2 and Im3 respectively.

The corresponding pixels on Im1, Im2 and Im3 are represented by three coordinate systems such as (x, y), (u, v) and (p, q). Here only the correction of Im2 with respect to Im1 has been described. The geometric correction of Im3 with respect to Im1 is done in the same manner. We try to find out two mapping functions f and g so that

$$u = f(x, y) \tag{1}$$

and

$$v = g(x, y) \tag{2}$$

Generally, the mapping functions are chosen as simple polynomials of first, second and third degree (Bernstein, 1983). We have taken third order polynomial in order to have a very precise alignment of two images in order to avoid any garbage change which might be detected at a later stage during

the change detection. The mapping functions are found as described below.

$$u = a_0 + a_1 x + a_2 y + a_3 xy + a_4 x^2 + a_5 y^2 + a_6 x^2 y + a_7 xy^2 + a_8 x^3 + a_9 y^3 \tag{3}$$

and

$$v = b_0 + b_1 x + b_2 y + b_3 xy + b_4 x^2 + b_5 y^2 + b_6 x^2 y + b_7 xy^2 + a_8 x^3 + b_9 y^3 \tag{4}$$

In order to find the coefficients a_i and b_i in the given equations, ten control points are chosen as there are 10 such coefficients. One must have the number of the equations equal to the number of the unknowns in order to find the unique solutions of the equations. However, in practice more control points than the minimum required number are chosen and coefficients are evaluated using least square estimation. This is how one builds up a geometrically rectified version of the image. The control points have been chosen in consultation with geologists. They are generally prominent features in the image such as bending, intersection points and so on. This is how Im2 is registered with respect to Im1. Similarly the registration of Im3 with respect to Im1 is done by finding two mapping functions h and k so that

$$p = h(x, y) \tag{5}$$
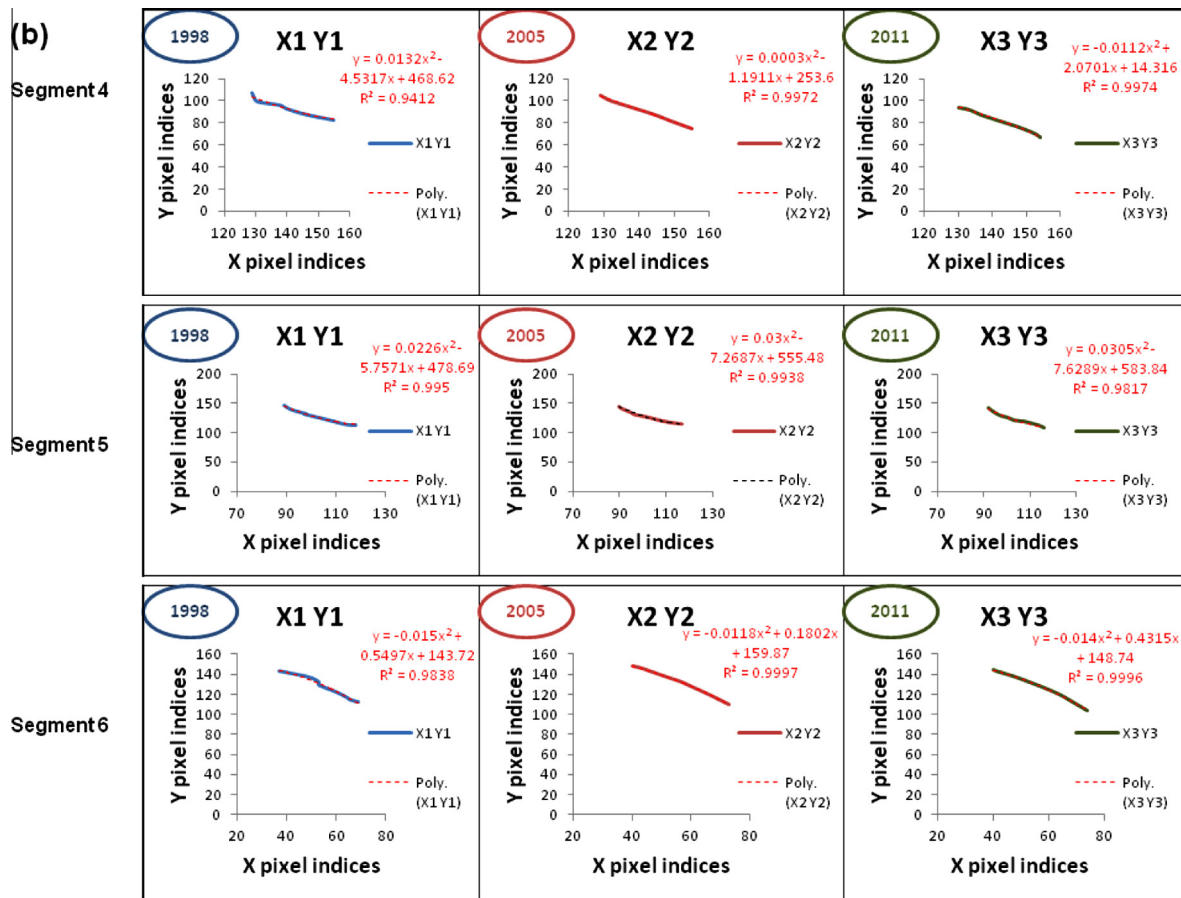
and

$$q = k(x, y) \tag{6}$$

Figure 8   Polynomial equations of the best fit curves for segments 4, 5 and 6 for each of the three years (1998, 2005 and 2011).

Table 1   Comparison of area change estimated by PCM and IM.

Seg. no.	Change in area occupied by glacier in pixels for segments						
	1998–2005			2005–2011			Increase/decrease in area in two timestamps (1998–2005) and (2005–2011)
	PCM	IM	Error	PCM	IM	Error	
1	80	73	7	60	65	5	Decrement
2	110	123	13	140	133	7	Increment
3	143	140	3	185	191	6	Increment
4	70	74	4	78	84	6	Increment
5	90	92	2	63	62	1	Decrement
6	45	44	1	36	33	3	Decrement

2.2.5. Skeleton formation and change detection

After registration, each image is processed to obtain skeletal edges using Canny's edge operator (Canny, 1986) for its robustness against noise and efficacy to detect true weak edges. Fig. 5 shows the typical skeletal images of the study region. In order to identify the prospective altered skeletal segments in the first time stamp (1998–2005), the skeletal image of the year 1998 has been XORed with the image of the year 2005 (Fig. 6(a)). Similarly, the skeletal image of the year 2005 has been XORed with the image of the year 2011 in order to identify the prospective altered skeletal segments in the second time stamp (2005–2011) (Fig. 6(b)). These two XORed images have also been further used for area calculation using PCM. XOR is a logical operation which produces a true value (one) when two of its inputs (the corresponding pixel values in two images) are different, indicating a change at the concerned pixel. If the two inputs are same then there will be a false (zero) at the output, indicating unchanged pixel.

2.3. Segment selection, modelling and area estimation

The choice of the segments is a trade-off between their lengths and contour complexities. The smoother the contour, the
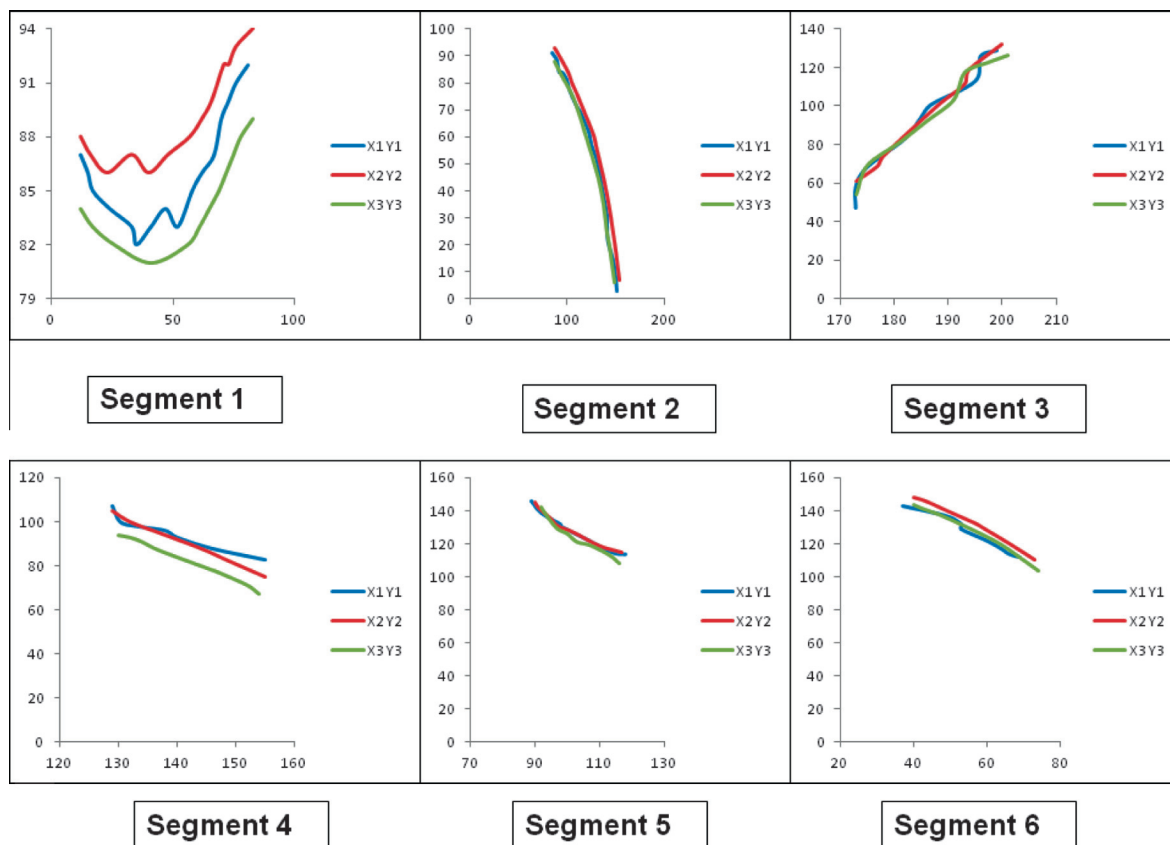
Figure 9 Enclosed differential areas in two timestamps (1998–2005) and (2005–2011).

larger is the segment length and vice versa. Further, choosing too many segments for the sake of accuracy is not advisable and the choice of optimum segments becomes difficult. Therefore the segments are chosen manually. These segments have been chosen in consultation with a geologist from the Wadia Institute of Himalayan Geology, Deharadun, India. Segment selection is a quite ticklish task here. Segments have been chosen with an idea that as long as the curve remains smooth or it does not involve too many zigzags then it keep on increasing the length of the segment. Otherwise restrict the length of the segment to small. The more complex the contour is the smaller will be segments in that region and vice versa. The whole process yields segments which can be mapped to a mathematical polynomial equation which describes the segment in a statistically optimal manner. The segment branches in the XORed images having significantly visible changes are identified first and regressed upon (using pixel indices) to derive polynomial equations.

To determine which mathematical equations model the dynamic surface in a statistically optimal way, polynomial regression model has been used (Carrara et al., 1991; Yuan and Bauer, 2007). Each of the identified branches are then further segmented such that the order of the functional equation (regression curve) for a particular segment in each of the original skeletal images does not go very high because the value of R^2 (Correlation Coefficient) does not change as significantly as the order of the curve after a particular order (Yuan and Bauer, 2007; Kim et al., 2012). This process yielded six segments of varying lengths as shown in Fig. 5.

Mathematical functional mapping was started with a liner equation and order of the equation was increased until a very optimal value of R^2 was achieved confirming the quality of the fit of the curve, however it was kept in mind that every increase in the order of the equation must cause a significant increase in the R^2 (Kumar et al., 2012). The polynomial equations for all the six segments for their best fit curves for each of the three years have been shown in Figs. 7 and 8 along with their R^2 values.

For area change estimation during the two time stamps, the modelled polynomial equations for each segment are superimposed on each other and the differential area enclosed amongst these curves are calculated using definite integrals using Eq. (7). In order to compare the results obtained by the proposed IM, the change in areas of all the segments has also been calculated by PCM (Sarkar and Chaudhuri, 1994) in the resulting image obtained after the XOR operation (see Fig. 6(a), (b)). Pixel counting method (PCM) involves counting the pixels which are enclosed between two polynomial equations of the same segment over two different time periods. Each pixel accounts for an area of 900 m^2. The net shift in area using PCM is calculated using Eq. (8). Both methods show quite similar results. Table 1 shows the results obtained by PCM and IM; and their comparisons in terms of absolute error for each of the six segments. Fig. 9 shows the enclosed differential areas in two timestamps (1998–2005) and (2005–2011) for all the six segments.

$$\text{Area} = \int (y1 - y2)dx \qquad (7)$$

$$\text{Net shift in area} = \text{Total no. of pixels} * 900 \, m^2 \qquad (8)$$

3. Results and discussion

For each segment, one can notice that the equation is a polynomial equation in nature and its coefficients are very random. Here glacier retreat is of our concern. Therefore the change being considered here is the change that is taking place at the bottom level of the glacier. As the glacier is melting along its edges, therefore the area occupied by the glacier is shrinking and the area not covered by the glacier is increasing. It can be seen from Table 1 that area occupied by the glacier has decreased in the second time stamp (2005–2011) in comparison to first time stamp (1998–2005) for segments 1, 5 and 6. However, one can notice that the rate of retreat of the glacier is higher in first timestamp and relatively lower in second timestamp in case of segments 1, 5 and 6. The segments 2 and 3 have shown an increase in area occupied by the glacier and segment 4 shows that there is almost no change as the change in area between two time stamps is very small. Therefore it is inferred that glacier is not at all retreating in the case of segments 2, 3 and 4. One of the possible reasons which can be cited here for the increase in area occupied by the glacier of segments 2 and 3 is the presence of a constant source of water below these segments, where water is getting frozen due to very low temperature of the concerned region and it is causing an increase in the area occupied by the glacier. Segments 1, 5 and 6 have shown a decrease in the second time stamp due to increased temperature caused by global warming. Based on the pattern being followed by the temperature of the concerned region, it is known that temperature has been increasing as verified by the Geological society of India. So we can say that temperature has played a vital role in the retreat of the segments 1, 5 and 6. As far as segments 2, 3 and 4 are concerned, we can only say that temperature effect has been over taken by some other factors say constant water source over there. The errors obtained for the area estimation by the two methods PCM and IM are very small as shown in Table 1 which fortify the applicability of the proposed method for the surface area estimation for glacier retreat application.

4. Conclusions

A novel technique for area change estimation has been applied to a severe glacial retreating zone. This technique can be used for its capability to measure the spatial and temporal changes in a glacial region and to subsequently determine effective means to measure glacier retreat. Estimation of water shortage or scarcity can be predicted based on stability of the segments. This technique can be employed for prediction and early warning systems of glacier retreat. The technique has been compared with the standard method of pixel counting and satisfactory results have been obtained. The accuracy of the proposed technique may further be improved by optimum selection of segments. However, optimum selection of the segments still remains a major challenge and needs further research. But it can definitely be taken as a reference for the particular path which might be followed by the particular glacier in the future and we can locate the vulnerable zones.

References

Asad Hakeem G.K., Gaurav Rajen M.V., 2007. Demilitarization of the siachen conflict zone: concepts for implementation and monitoring. Sandia Report, SAND 2007–5670, Sandia National Laboratories, September 2007, Albuquerque, NM.

Bamber, J.L., Rivera, A., 2007. A review of remote sensing methods for glacier mass balance determination. Global and Planetary Change 59 (1–4), 138–148.

Bartholom, A.E., Belward, A.S., 2005. GLC2000: a new approach to global land cover mapping from Earth observation data. International Journal of Remote Sensing 26 (9), 1959–1977.

Bernstein, R., 1983. Image Geometry and rectification. Manual of remote sensing. American Society of Photogrammetry 1, 875–881.

Berthier, E., Arnaud, Y., et al, 2007. Remote sensing estimates of glacier mass balances in the Himachal Pradesh (Western Himalaya, India). Remote Sensing of Environment 108 (3), 327–338.

Bishop, M.P., Shroder Jr., J.F., et al, 2007. 25 Remote sensing and GIS for alpine glacier change detection in the Himalaya. Developments in Earth Surface Processes, Elsevier 10, 209–234.

Bolch, T., Menounos, B., et al, 1985. Landsat-based inventory of glaciers in western Canada, 1985–2005. Remote Sensing of Environment 114 (1), 127–137.

Canny, J., 1986. A computational approach to edge detection. Pattern Analysis and Machine Intelligence IEEE Transactions on PAMI 8 (6), 679–698.

Carrara, A., Cardinali, M., et al, 1991. GIS techniques and statistical models in evaluating landslide hazard. Earth Surface Processes and Landforms 16 (5), 427–445.

Coppin, P.R., Bauer, M.E., 1996. Digital change detection in forest ecosystems with remote sensing imagery. Remote Sensing Reviews 13, 207–234.

Coppin, P., Jonckheere, I., et al, 2004. Review article digital change detection methods in ecosystem monitoring: a review. International Journal of Remote Sensing 25 (9), 1565–1596.

Gonzalez, R.C., Woods, R.E., Eddins, S.L., 2009. Digital Image Processing Using MATLAB. Gatesmark Publishing.

Gupta, K.R., 2008. Global Warming (Encyclopaedia of Environment). Atlantic Publishers and Distributors.

IPCC, 2007. IPCC Fourth Assessment Report: Climate Change 2007. 2012, from <http://www.ipcc.ch/publications_and_data/ar4/wg1/en/ch4s4-1.html>.

Kapadia, H., 1998. Meeting the Mountains. Indus Publishing Company.

Karimi, N., Farokhnia, A., 1955. Elevation changes of Alamkouh glacier in Iran since 1955, based on remote sensing data. International Journal of Applied Earth Observation and Geoinformation 19, 45–58.

Khromova, T.E., Osipova, G.B., et al, 2006. Changes in glacier extent in the eastern Pamir, Central Asia, determined from historical data and ASTER imagery. Remote Sensing of Environment 102 (1–2), 24–32.

Kim, Y., Kimball, J.S., et al, 2012. Satellite detection of increasing Northern Hemisphere non-frozen seasons from 1979 to 2008: implications for regional vegetation growth. Remote Sensing of Environment 121, 472–487.

Klein, A.G., Isacks, B.L., 1999. Spectral mixture analysis of Landsat thematic mapper images applied to the detection of the transient snowline on tropical Andean glaciers. Global and Planetary Change 22 (1–4), 139–154.

Kumar, P., Bhondekar, A.P., et al, 2012. Modelling and estimation of spatiotemporal surface dynamics applied to a middle Himalayan region. International Journal of Computer Applications, Foundation of Computer Science, New York, USA 54 (7), 8.

Mas, J.F., 1999. Monitoring land-cover changes: a comparison of change detection techniques. International Journal of Remote Sensing 20 (1), 139–152.

Mihalcea, C., Brock, B.W., et al, 2008. Using ASTER satellite and ground-based surface temperature measurements to derive supra-glacial debris cover and thickness patterns on Miage Glacier (Mont Blanc Massif, Italy). Cold Regions Science and Technology 52 (3), 341–354.

Moholdt, G., Nuth, C., et al, 2010. Recent elevation changes of Svalbard glaciers derived from ICESat laser altimetry. Remote Sensing of Environment 114 (11), 2756–2767.

Moran, D., 2011. Climate Change and National Security: A Country-Level Analysis. Georgetown University Press.

Paul, F., Huggel, C., et al, 2004. Combining satellite multispectral image data and a digital elevation model for mapping debris-covered glaciers. Remote Sensing of Environment 89 (4), 510–518.

Paul, F., Kaab, A., et al, 2007. Recent glacier changes in the Alps observed by satellite: consequences for future monitoring strategies. Global and Planetary Change 56 (1–2), 111–122.

Rao, Y.S., 2011. Synthetic Aperture Radar Interferometry for Glacier Movement Studies. Springer.

Richards, J.A., Jia, X., 2010. Remote Sensing Digital Image Analysis. Springer (India) Private Limited, New Delhi, India.

Sadangi, H.C., 2007. India's Relations with Her Neighbours. Isha Books.

Sarkar, N., Chaudhuri, B.B., 1994. An efficient differential box-counting approach to compute fractal dimension of image. Systems, Man and Cybernetics, IEEE Transactions on 24 (1), 115–120.

Sawaya, K.E., Olmanson, L.G., et al, 2003. Extending satellite remote sensing to local scales: land and water resource monitoring using high-resolution imagery. Remote Sensing of Environment 88 (1–2), 144–156.

Singh, A., 1989. Review article digital change detection techniques using remotely-sensed data. International Journal of Remote Sensing 10 (6), 989–1003.

Venteris, E.R., 1999. Rapid tidewater glacier retreat: a comparison between Columbia Glacier, Alaska and Patagonian calving glaciers. Global and Planetary Change 22 (1–4), 131–138.

Warning, G.G., 2012. Glacial Retreat. from: <http://www.global-greenhouse-warming.com/glacial-retreat.html>.

Yuan, F., Bauer, M.E., 2007. Comparison of impervious surface area and normalized difference vegetation index as indicators of surface urban heat island effects in Landsat imagery. Remote Sensing of Environment 106 (3), 375–386.